
Jigsaw: A Foliage-Penetrating 3D Imaging Laser Radar System

Richard M. Marino and William R. Davis, Jr.

■ Situation awareness and accurate target identification are critical requirements for successful battlefield management. Ground vehicles can be detected, tracked, and imaged by using airborne or space-borne microwave radar. Obscurants, however, such as camouflage net and tree-canopy foliage can degrade the performance of these radars. Foliage can be penetrated with long-wavelength microwave radar, but generally at the expense of imaging resolution. The DARPA Jigsaw program includes the development of high-resolution three-dimensional (3D) imaging laser radar (ladar) sensor technology and systems that can be used in airborne platforms to image and identify military ground vehicles hiding under camouflage or foliage. Lincoln Laboratory has developed a rugged and compact 3D imaging ladar system that successfully demonstrates this application. The sensor system, including a microchip laser and novel focal-plane arrays, has been integrated into a UH-1 helicopter. The sensor operates day or night and produces high-resolution 3D spatial images by using short laser pulses and a focal-plane array of 32×32 Geiger-mode avalanche photodiode (APD) detectors with independent digital time-of-flight counting circuits at each pixel. With appropriate optics, the 32×32 array of digital time values represents a 3D spatial image frame of the scene. Successive image frames from the multi-kilohertz pulse-repetition-rate laser pulses are accumulated into range histograms to provide 3D volume and intensity information. In this article, we describe the Jigsaw program goals, our demonstration sensor system, and the data-collection campaigns, and we show examples of 3D imaging with foliage and camouflage penetration. Other applications for this 3D imaging direct-detection ladar technology include robotic vision, navigation of autonomous vehicles, manufacturing quality control, industrial security, and topography.

THERE ARE MANY IMPORTANT applications for optical detectors that are sensitive enough to measure individual photons. Generally, optical sensors and communication systems can be made more efficient in power and volume by using photon-counting receivers. These receivers may require narrow spatial, temporal, and/or spectral filters to reduce unwanted background noise or clutter. Active sensors—those using lasers for illumination—can be made more sensitive and signal-efficient by tuning the receiver filters to the narrow spatial, temporal, and/or spectral features of

the laser transmitter. High-resolution three-dimensional (3D) spatial imaging is one application of significant interest.

The Defense Advanced Research Projects Agency (DARPA) and the U.S. Army have a joint vision for future combat systems that utilize sensor and information networks [1]. One of the primary goals of these systems is to increase force survivability through robust situation awareness, accurate target identification, and rapid response to tactical threats. Relatively small, unmanned air vehicles (UAV) will be used with a variety of active

and passive sensors to collect information and imagery. High-resolution 3D imaging laser radar (ladar) can provide object and scene imagery with sufficient quality for human analysts to perform object classification and identification. UAV payload constraints, however, impose limitations on sensor size, weight, and power requirements. The endurance and range of UAV platforms will increase with relatively low-weight, more efficient payloads. The missions of future combat systems will require compact, lightweight, and power-efficient ladar systems to provide high-resolution 3D imagery.

Lincoln Laboratory has been developing high-resolution ladar sensors and technology since the 1970s [2]. Recent developments of compact solid-state microchip lasers and high-efficiency Geiger-mode avalanche photodiode (APD) detector arrays have enabled the development of compact and rugged ladar sensor systems [3–5]. In this article, we report on the DARPA-funded Jigsaw ladar sensor technology, the functional prototype system, and airborne field-test demonstrations.

Goals of the Jigsaw Program

Military ground vehicles located in the open can be detected, tracked, and imaged by using airborne or space-borne microwave radar. Obscurants, however, such as camouflage net and foliage such as tree canopy can degrade the imaging and tracking performance of such radars. Accurate and timely target identification are required by the future combat systems program in order to maximize targeting efficiency. The goals of the DARPA Jigsaw program include the development and demonstration of high-resolution 3D imaging laser radar (ladar) sensor technology, techniques, and systems that could be used from unmanned airborne platforms to image and identify military ground vehicles hiding under camouflage or foliage such as tree canopy.

From any single viewing direction above the ground surface, the laser illumination pattern may be obscured by more than 95% in area and result in a very sparse sampling of the scene below the obscurant. The operational theory is that if the angle-angle-range-resolved data points could be collected from a diversity of angular viewing directions, then perhaps they could be combined, as in a 3D jigsaw puzzle, to provide a sufficient number of target surface samples or density to support accurate and reliable target identification. Pre-

vious studies in target recognition using high-resolution imagery led to the Jigsaw sensor resolution or volume image sampling goal of three-inch (or 7.5 cm) cubic voxels [6].

The Jigsaw concept of operations includes a sequence of events that begins with a handover or queue of a specified geolocation (assumed to be accurate to ± 10 meters), possibly within a stand of trees, where a suspect object or unidentified vehicle has been detected. The airborne platform flies to the given geolocation, initiates the ladar sensor, and collects 3D data while passing over the target location. The sensor line of sight is directed at the target location area throughout the pass in order to collect the necessary diversity of viewing directions. If needed, registration algorithms are used to combine the data taken from the various viewing directions. The goal is for total latency in fifteen minutes, including data acquisition, data and image processing, data transmission from airborne platform to ground station computers, and image visualization at a ground station. A companion article in this issue, entitled “Simulation of 3D Laser Radar Systems,” by Michael O’Brien and Daniel G. Fouche, describes the measurement simulations and performance metrics of the Jigsaw sensor system.

Under DARPA support a team was formed with staff from Lincoln Laboratory, Harris Corporation, and Sarnoff Corporation to develop the sensor system, data processing algorithms, and visualization applications to demonstrate the Jigsaw system utility and capabilities in a realistic environment. Although the three organizations worked together as a team, principal responsibilities were more specialized. Lincoln Laboratory provided the ladar sensor system, data processing for raw-to-3D frame formation, and onboard electronics and operators. Sarnoff Corporation developed rapid 3D registration algorithms. Harris Corporation served as overall system integrator, and provided the wireless communication system and the ground data processing system, visualization tools, and operators.

In particular, the goal was to demonstrate the feasibility to perform human-based target identification of ground vehicles under foliage and camouflage obscurants with data collected from an airborne platform (a manned UH-1 helicopter) operating at speeds and altitudes similar to those expected for future operational

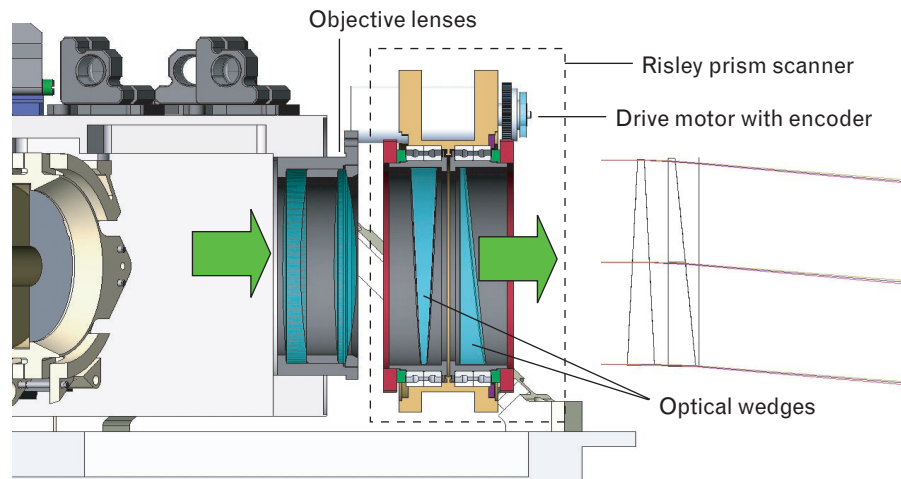


FIGURE 1. The Risley prism scanner mechanism. The instantaneous field of regard of the Jigsaw sensor is narrow; the 32×32 focal-plane array covers an area only two meters square at a range of two hundred meters. The front-end optics include a compact scanner subsystem—the Risley prism pair—consisting of two counter-rotating optical wedges or prisms. This scanner increases the field of regard to cover a 37-meter-diameter circle at a range of two hundred meters. Each prism has an independent drive motor and controller.

lightweight UAVs. The demonstration goals for data collection included single-pass data collections from an altitude of a hundred or more meters above ground level, ground-target acquisition area of twenty meters square, aircraft ground speed of twenty-five to thirty-five meters per second, and day or night operation.

Another important program goal was to collect flight data by December 2002, within six months of the start of the effort. Because of this tight time restriction, the schedule drove us to utilize proven or heritage technology and well-defined approaches whenever applicable in order to minimize the risk of unexpected complications and delays.

Sensor Requirements and Design Tradeoffs

The sensor and system design requirements flow down from the higher-level program goals. For example, the sensor field of regard and cross-range resolution requirements lead to the ideal focal-plane-array size of greater than 256×256 to cover the 20-m field with 7.5-cm samples. However, the largest and most mature Geiger-mode APD arrays were processed in silicon with 32×32 pixels on $100\text{-}\mu\text{m} \times 100\text{-}\mu\text{m}$ pitch. Thus the 32×32 array provided an instantaneous field of view of only 10.1×10.1 mrad, which satisfied the 7.5-cm (or less) cross-range resolution requirement.

The limited size of available detector arrays required the inclusion of beam pointing or scanning. We developed a relatively compact scanning system called a Risley prism scanner, based on a pair of counter-rotating optical wedges or prisms. Although a wide variety of scan patterns could be achieved with two independent motor drivers, we chose to limit the scope to a constant motor rate and low-power operation. Figure 1 illustrates the Risley prism scanner. Figure 2 shows an example of the scan patterns that are achieved with this scanner in durations of 0.25, 0.5, 1.0, and 1.39 sec. The envelope of the scan pattern covers the required twenty-meter-square acquisition area from a nominal range of 150 m. The diameter of the overall circular field of regard is 10.8° (0.19 rad).

The Jigsaw lidar sensor required high sensitivity for the lidar backscattered signal with minimal sensitivity to solar-illuminated background light. The optical design took advantage of the relatively low fill factor of the focal-plane array. The detector pixel active area is about thirty microns in diameter, so the effective fill factor of the array is only about 7% by area. We could increase the fill factor by bonding a microlens array to the detector array, but this would also increase the background light flux by more than a factor of ten. We chose an alternative and proven approach to increase the optical

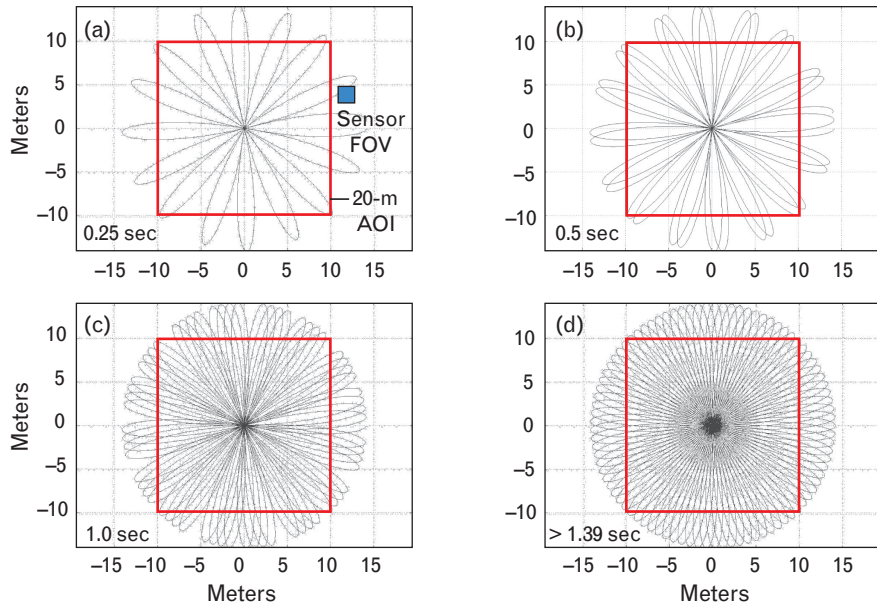


FIGURE 2. Examples of Risle scan patterns over four different time durations. To emulate a low-power Risle scanner, the two prisms in the Jigsaw sensor are rotated at constant but different rates. The line-of-sight axis of the Jigsaw sensor produces a rosette pattern when the two Risle prisms are rotating in opposite directions. The arms of the scan pattern rotate and sample the field of regard with increasing density over time. The sampling density is highest in the center of the scan pattern. The blue square in part a shows the instantaneous field of view (FOV) of the Jigsaw sensor. The red square illustrates the required twenty-meter-square area of interest (AOI) covered by the scan pattern from a nominal altitude of 150 m above the ground.

coupling and reduce background flux. The optical architecture of the Jigsaw sensor is similar to that of the proven Gen-III design [5]; both systems used a diffractive optical element from MEMS, Inc., to transform the single-mode laser beam (TEM_{00}) into a far-field 32×32 spot pattern, as illustrated in Figure 3. Each pixel of the detector array is aligned to its respective laser beamlet. Maintaining the alignment between the receiver and transmit paths to keep the laser spots aligned with the individual detector pixels (or dots) proved to be the most challenging aspect of the optical design and implementation. Figure 4 illustrates the transmit and receive optical paths of the Jigsaw ladar sensor, with the transmit path in red and the receive path in green.

The helicopter flight environment required maintaining optical alignment over a temperature range of -10° to $+40^\circ\text{C}$ while the sensor was subjected to helicopter-induced vibration. Super-Invar was selected as the material for the optical bench and main structure because of its extremely low thermal expansion coefficient over this temperature range. The most sensitive elements of the optical train for spots-to-dots alignment

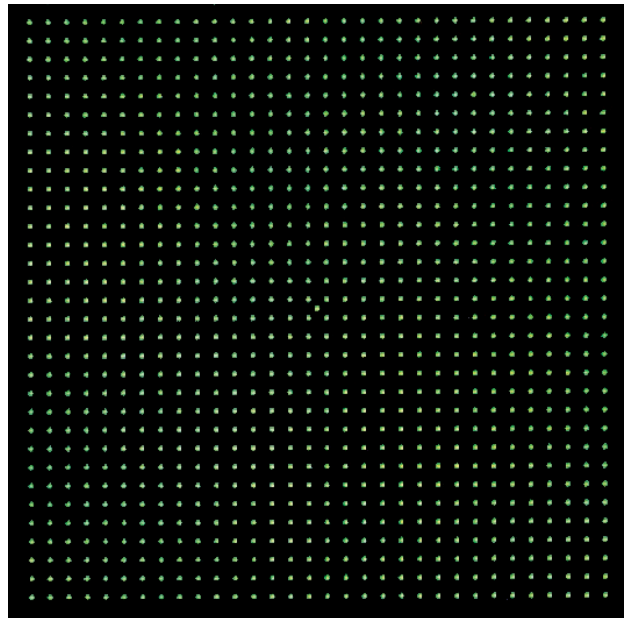


FIGURE 3. A photograph of the far-field 32×32 laser spot pattern. The transmit optics include a diffractive optical element that transforms the single Gaussian laser beam profile into a 32×32 array of beamlets. Each spot was aligned to an individual detector in the 32×32 focal-plane array.

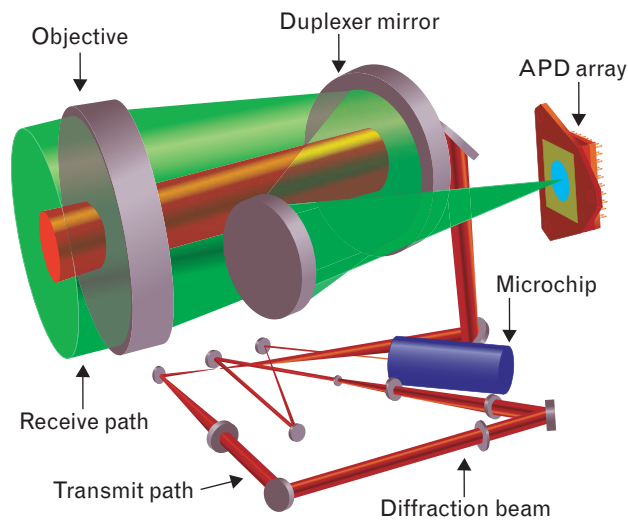


FIGURE 4. An illustration of the transmit (red) and receive (green) optical paths in the Jigsaw sensor. The size of the sensor is constrained to fit within the inner yoke of a thirty-inch gimbal mount. The optical design is made compact by using a common objective lens, folded optical paths, and a custom optical support structure.

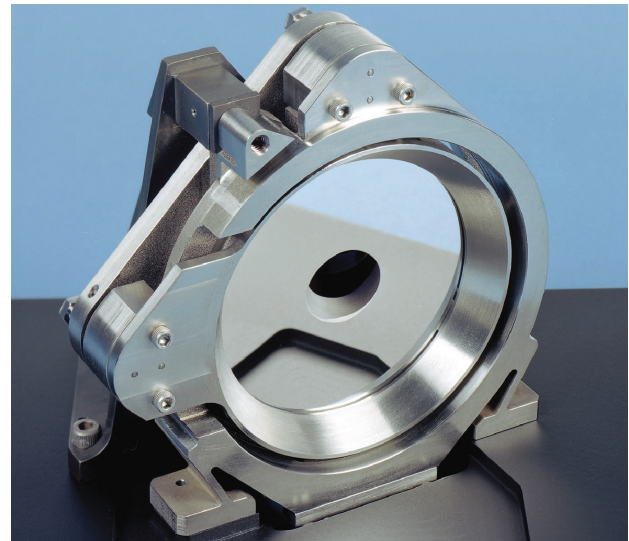


FIGURE 5. The duplexer mirror in its titanium mount. The mirror is designed to maintain alignment of the transmit spots and detector pixels over a wide temperature range and in helicopter vibration conditions. The mirror mount was machined from a single block of titanium, and includes flexures for thermal expansion and alignment.

Table 1. Jigsaw Ladar Sensor System Parameters

<i>Parameter</i>	<i>Value</i>	<i>Comment</i>
Nominal range	150 m	
Field of regard	10.8°	28.3 m diameter at 150 m range
Laser wavelength	532 nm	
Laser far-field beam pattern	32 × 32 spot array	Aligned with detector array
Laser pulse width	300 psec	Full width half max
Laser pulse and raw imaging rate	16,000 per sec	
Receive aperture diameter	7.5 cm	
Effective focal length	300 mm	
Focal ratio	<i>f</i> /4.0	
Number of pixels in focal-plane array	32 × 32	
Projected 100- μ m pixel pitch	333 μ rad	
Instantaneous cross-range sample	5 cm at 150 m range	< 7.5 cm goal
Field of view (32 × 32)	10.1 mrad × 10.1 mrad	
Range resolution	40 cm	> 7.5 cm goal
Focal-plane array range sampling rate	2 GHz effective	500 GHz plus two vernier bits
Instantaneous field of regard	10.1 mrad × 10.1 mrad	1.51 m square at 150 m range (32 × 32 array)

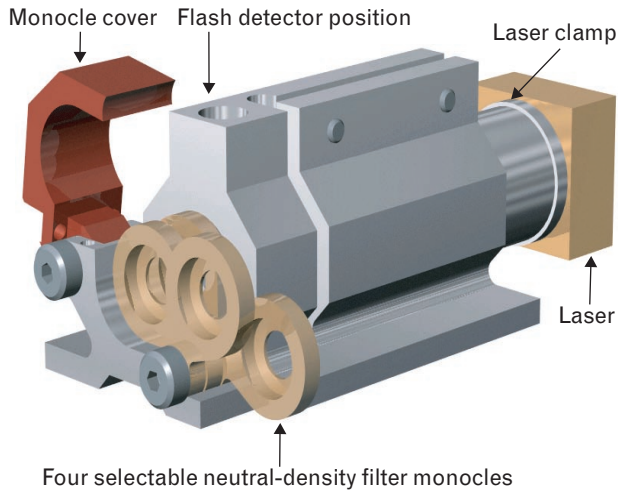


FIGURE 6. A model of the microchip laser head assembly, showing the four selectable neutral-density filters. The filters are used to adjust the transmit pulse energy in order to operate the sensor in the photon-counting mode. The flash detector is used to measure the precise time when each laser pulse fires.

were the duplexer and turning mirrors in the receive optics. Titanium was chosen for these mirror mounts as the best compromise between required thermal properties and stiffness. To provide fine adjustment capability while maintaining high stiffness, each mirror mount was machined from a single blank of titanium including integral two-axis flexures. Figure 5 shows an illustration of the duplexer mirror, its titanium mount, and the alignment adjustment screws. Table 1 lists the key Jigsaw sensor parameters.

Sensor Design and Technology

The Jigsaw sensor uses Lincoln Laboratory–developed microchip laser technology. The microchip laser is a passively *Q*-switched solid-state frequency-doubled Nd:YAG laser that transmits short laser pulses (300 psec full width half maximum) at a pulse rate of 16 kHz and at a wavelength of 532 nm. The laser was packaged in a head assembly along with a set of four selectable neutral-density filters, as illustrated in Figure 6. A small portion of the laser pulse energy is directed to a linear positive intrinsic negative (PIN) photodiode located within the laser mount. The signal from this flash detector is used to initiate the timing circuits of the Geiger-mode APDs for each laser pulse.

The Jigsaw sensor uses a novel photon-counting de-

tor technology, also developed at Lincoln Laboratory [3]. The focal-plane array is comprised of photon-counting Geiger-mode APDs with digital time-of-flight counters at each pixel. The single-photon detection efficiency was measured to be greater than 20% when using the 32×32 silicon Geiger-mode APDs at room temperature. In Geiger-mode operation, the APD saturates while providing a typical gain greater than 10^8 . The pulse out of the detector is used to stop a digital clock register integrated within the focal-plane array at each pixel. The time of flight is measured independently for each pixel with a timing quantization of 500 psec (2-GHz effective clock rate). Using the detector in this binary response mode simplifies the signal processing by eliminating the need for analog-to-digital converters and non-linearity corrections. The 32×32 array of digital time values represents a 3D spatial image frame of the scene for each laser pulse. The APD detector array with integral electronics was mounted on a small thermoelectric cooler that maintained the detector at a constant near-room temperature. Figure 7 shows the detector-cooler combination. The complete detector package

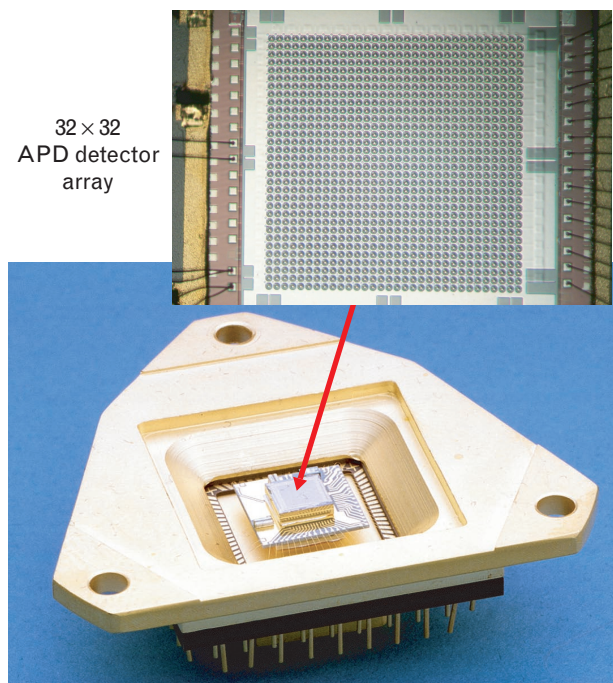


FIGURE 7. The 32×32 Geiger-mode avalanche photodiode (APD) detector array, mounted on a thermoelectric cooler. This unit was hermetically sealed into a detector package to stabilize the detector’s operating temperature near 20°C.

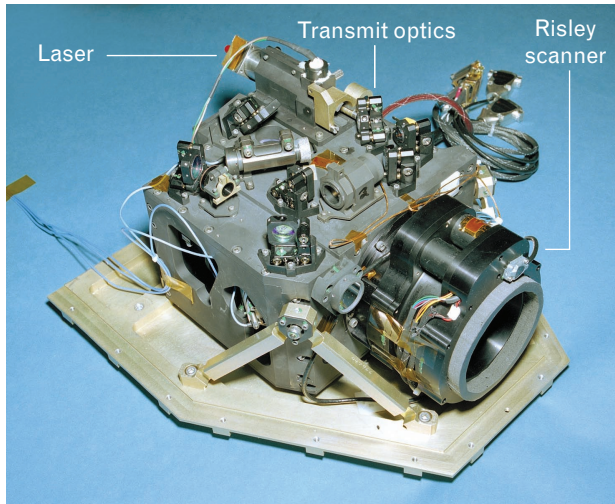


FIGURE 8. The Jigsaw sensor optical head, with all components integrated into a compact and rugged sensor system.

is hermetically sealed for protection, and includes a sapphire window (not shown in this photograph).

The Risley prism scanner uses two counter-rotating prisms, one rotating at 36 Hz and the second at 28 Hertz. Optical encoders are used on the two independent scanner motors to record the precise viewing direction for each laser pulse.

The laser, detector array, Risley scanner, and transmit-receive optics were assembled into the sensor optical unit shown in Figure 8. As mentioned earlier, the basic structural box, or optical bench, was made of Invar. The laser and transmit optics are on top of the structure. The transmit beam is directed down into the interior of the box and out through the duplexer, objective lenses, and scanner. The receive optics are inside the box. The detector package is hidden from view on the back of the box. A focal-plane readout and timing circuit board was removed for clarity. This sensor design, while relatively heavy at 13.6 kg, proved to be the most expeditious approach to meeting a demanding development schedule.

The schedule necessitated the use of rapid prototyping techniques as much as feasible. Common databases facilitated rapid iterations and data exchanges between computer-aided design (CAD), structural and thermal analysis, and optical ray-tracing computational tools to finalize the design. Rapid prototype models of the duplexer and Risley prism mechanism also facilitated the design and fabrication process.

Lincoln Laboratory also developed the electronic subsystems used to read out the focal-plane array data at 32 MB/sec and record the raw data along with sensor and platform state data onto RAID disks. Two dual-Pentium IV processors were integrated into the flight electronics racks. One processor pair provided onboard operator interfaces to control and monitor the sensor state, laser operations, and data acquisition and recording. The second processor pair was used to perform low-latency onboard data processing, to monitor the state of the Applanix 310 Global Positioning System (GPS) inertial navigation system (INS), and to display and record passive video imagery from an Indigo uncooled micro-bolometer long-wave infrared (LWIR) camera.

Data Processing

In addition to the sensor system and data-acquisition system, Lincoln Laboratory developed algorithms to combine the raw angle-angle-range data and time data with the GPS/INS information and the pointing data from our Risley scanners to transform the 3D data points into xyz geolocated coordinates. As anticipated, linear and angular velocity errors in the GPS/INS blended solution restricted the time over which 3D data could be accumulated before image spatial blurring became unacceptable.

Successive image frames from the 16-kHz pulse-repetition-rate laser pulses were accumulated into spatially resolved histograms to provide 3D volume and intensity information. Typically, raw data sets were transformed into xyz coordinates and accumulated for a duration of 0.25 sec. The 3D data points were spatially filtered by applying thresholds to either range histograms or xyz voxel histograms. Sarnoff Corporation and Harris Corporation developed 3D-data frame registration and filtering algorithms that were used during flight tests to demonstrate low-latency data processing. Harris Corporation also developed applications for visualization and mensuration to support identification decisions by a human analyst. Typically, the object length, width, and surface structure were used as signatures for identification.

Another companion article in this issue, entitled "Pose-Independent Automatic Target Detection and Recognition Using 3D Laser Radar Imagery," by Alexandru N. Vasile and Richard M. Marino, describes

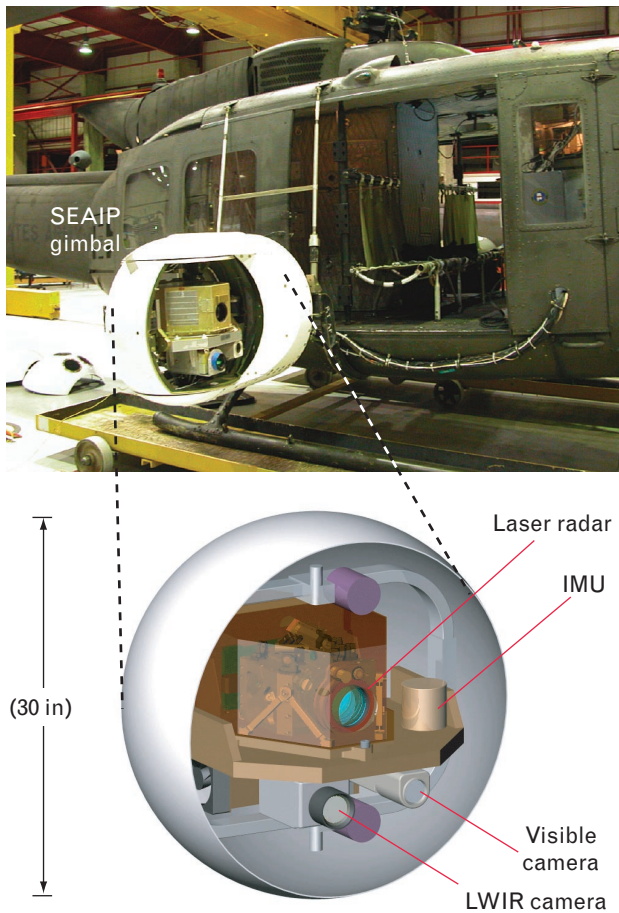


FIGURE 9. The UH-1 helicopter with the Stabilized Electro-Optical Airborne Instrumentation Platform (SEAIIP) gimbal and the Jigsaw imaging sensor payloads. The Jigsaw sensor was integrated into the 30-in diameter gimbal along with an inertial measurement unit (IMU), a visible camera, and a long-wave infrared (LWIR) camera. The SEAIIP gimbal provided line-of-sight pointing at specified geolocations that were selected before each flight.

the development of automatic target detection and recognition algorithms, and their application to 3D lidar imagery.

Airborne Data-Collection Campaigns

The Jigsaw system was tested and demonstrated during winter (December 2002 to February 2003) and summer (June to July 2003) data-collection campaigns. The Army Redstone Technical Test Center (RTTC) at Redstone Arsenal in Huntsville, Alabama, provided the test range, the ground vehicle targets and surveys, the UH-1 helicopter and pilots, and flight and test support. Southern Research Institute (SRI) developed a stabi-



FIGURE 10. Ground vehicles with camouflage and foliage obscurants at the Army Redstone Technical Test Center in Huntsville, Alabama. These vehicles and others were placed in various scenes for 3D imaging tests, including in the clear, within a stand of trees, at the edge of a tree line, and both with and without camouflage net obscurants.



FIGURE 11. Photographs of winter foliage (top) and much denser summer tree-canopy foliage (bottom), taken during the winter and summer lidar data-collection campaigns in Huntsville, Alabama.

lized thirty-inch-diameter, four-axis gimbal known as the Stabilized Electro-Optical Airborne Instrumentation Platform (SEAIP). With the SEAIP mounted on the side of the UH-1 helicopter, RTTC provided a valuable and general-purpose airborne platform testbed.

SRI also developed a new GPS tracking capability for the Jigsaw program. In this mode, the SEAIP controller used site-provided real-time differential global positioning system (DGPS) error corrections with a Litton LN200 Inertial Measurement Unit (IMU) and an Applanix 310 INS to point the SEAIP gimbal at a given or known target ground location, regardless of the UH-1 location, vibrations, or flight attitude. Figure 9 shows a photo of the SEAIP gimbal mounted to the UH-1 platform, and an illustration of the components inside the gimbal.

Ground vehicles were placed in a variety of scenes with varying amounts of natural obscuration, including in the clear, adjacent to a stand of trees, in a tree stand

on a dirt road, and in a tree stand off the road. Target geolocations were predetermined by using stationary GPS receivers and ground surveys. Preflight planning included selection and sequence of predetermined ground target locations and flight paths. Figure 10 shows photographs of a few examples of ground vehicles used during the summer and winter campaigns.

Figure 11 shows photographs of typical scenes of winter and summer foliage, taken from the air during the winter 2002 and 2003 summer campaigns. The tree canopy was quite thick in the summer, and the UH-1 pilots had difficulty locating the ground vehicles underneath. The natural mixed-conifer foliage produced an effective obscuration of the ground vehicles that ranged from 35% to 75% in the winter, and from 70% to 92% in the summer. The camouflage netting used on the vehicles was a standard military single-layer summer-woodland type of material with about 50% obscuration.

The concept of operations included collecting lidar data during a single overhead pass from an altitude of normally 150 meters above ground level. During a typical flight, data were collected from about six target locations, with a total of twenty to forty overflight passes. As the airborne platform approached the target volume of interest, the SEAIP gimbal was controlled to point at a measured or known geolocation on the ground, in the so-called GPS tracking mode. Data were collected with ground vehicles in each of these scenes and both with

Table 2. Target Types

<i>Target</i>	<i>Country</i>
T72 tank	Russia
M60 tank	U.S.
M2A3 Bradley fighting vehicle	U.S.
M1A1 Abrams tank	U.S.
BMP-1 armored personnel carrier	Russia
BTR-70 armored personnel carrier	Russia
HMMWV truck	U.S.
M35 2½-ton truck	U.S.
Standard green truck (calibration target)	U.S.

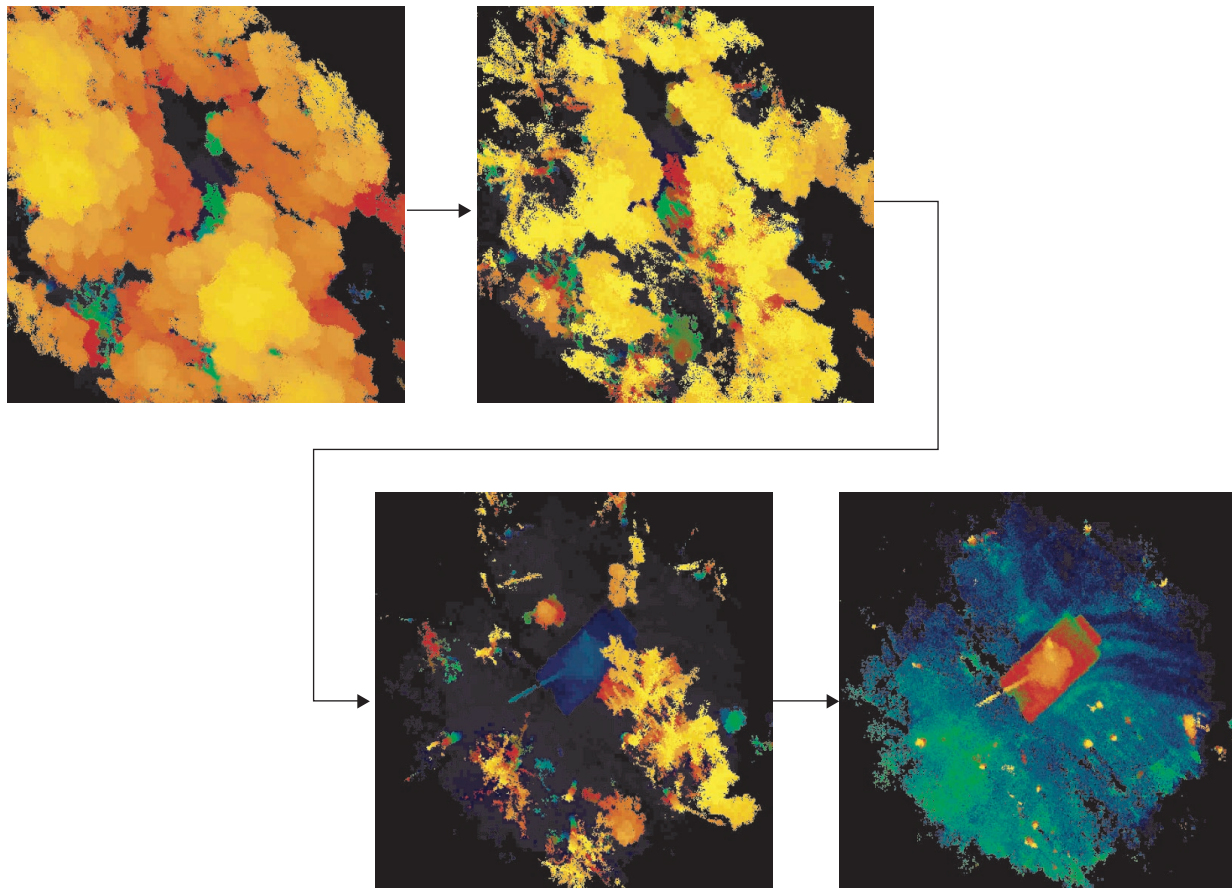


FIGURE 12. Sequence of 3D images with color-coded height and canopy removal via color-bar compression. Once the raw angle-angle-range data are collected and processed into 3D point clouds, they can be displayed with color representing relative height. This sequence of images shows the effect of cropping the 3D data by successively compressing the color bar used in the computer display. The first image (upper left) shows the tree tops and the fourth image (lower right) shows the 3D scene below the tree canopy. The tank is clearly revealed, along with the tree trunks, in the fourth image.

and without camouflage net in place above the vehicles. The duration of a typical flight test was limited to about two hours by the fuel capacity of the UH-1 helicopter.

During the winter data-collection campaign, lidar and infrared (IR) passive imagery was collected from ten flights and more than 190 overflight passes. During the summer campaign, data were collected from seven flights and more than 200 overflight passes. Table 2 lists a variety of ground vehicles that were used for the data-collection campaigns.

Examples of 3D Imagery

We demonstrate the imaging quality we achieved by showing the 3D imagery we collected in a variety of collection geometries and various amounts of obscuration. Although imagery was collected from all of the

targets listed in Table 2, a small subset of the 3D imagery collected can illustrate the imaging quality. Perhaps the best way to observe the 3D image data is with a dynamic viewer, which allows the user to view the 3D data set from any perspective or distance. Print publications, however, do not (yet) have the capability to display dynamic data. Instead, Figure 12 shows a series of still images that were selected from a dynamic 3D data display. Here the color code represents the height above the ground, and the mapping of height to color is chosen to effectively crop off the obscuring tree tops above the tank. All the image data are projected for a viewing perspective above the vehicle. Figure 13 shows the same vehicle from an off-nadir and closer perspective. Some tree trunks appear in the scene, since they are within the height band selected for color rendering.

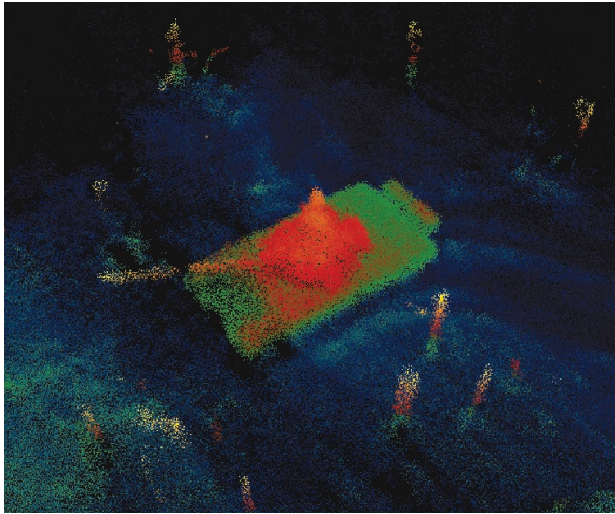


FIGURE 13. Perspective view of color-coded 3D image data of a tank. One of the features of 3D spatial imagery is the freedom to display the data from any perspective and to zoom in on areas of interest. This figure shows a perspective view of the data in the fourth image of Figure 12. The structure of the tank can be recognized as well as tread marks in the soil. Tree trunks also appear in the scene because they occupy the same color height band as the tank.

Figure 14 shows examples of high-resolution 3D imagery below summer foliage for four different vehicle scenes. The tree canopy has been effectively removed from the display by compressing the height-coded color band. The unambiguous metric and spatial structure of these vehicles are clearly observable and can be used for human-based or machine-based identification. An open hatch can be seen in the tank on the right.

Figures 15 and 16 show an example of 3D imagery of a vehicle (or something) under camouflage net and summer tree canopy. Again, the color coding represents height above ground for a slice of data that includes the target and ground, but excludes the trees above. In Figure 16 the upper bound of the selected data slice was adjusted to reveal the target vehicle just below the camouflage net.

Figure 17 shows a 3D image of a storage-yard scene that includes ground vehicles and small buildings. The data were recorded with the platform at an altitude of approximately 450 m and the field of regard covered a circular area of about 85 m in diameter. Figure 18

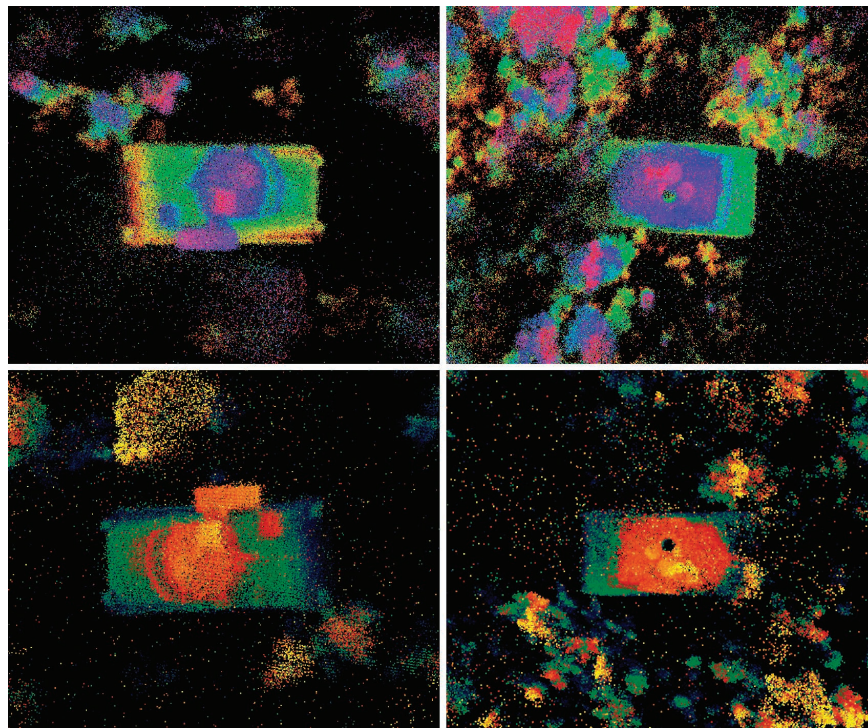


FIGURE 14. Examples of high-resolution 3D imagery below summer foliage for four different vehicle scenes. The tree canopy has been removed from the display by compressing the height-coded color band. The spatial structure of these vehicles are clearly observable and can be used for identification. An open hatch can be seen in the tank on the right.

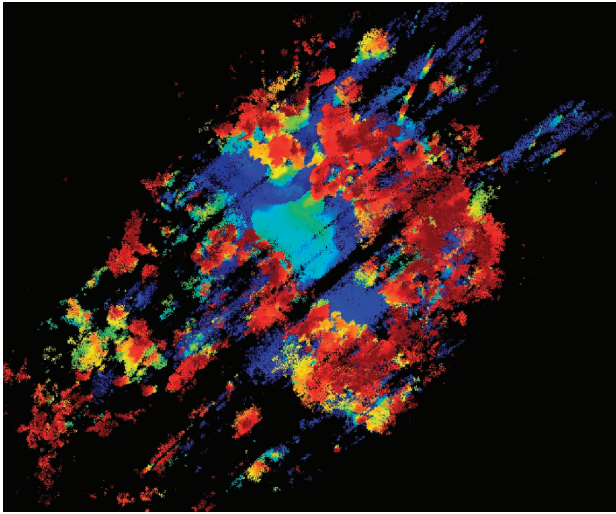


FIGURE 15. A 3D image of a scene with a vehicle on a dirt road under summer tree foliage and under camouflage net. The height axis is again color coded in this display, and some of the tree canopy has been removed by compressing the color bar. The camouflage net is in the center of the scene, and is colored light blue.

shows a small subset of the larger data set, where the display provides a close-in perspective of the tank and truck near the center of the storage-yard scene.

Summary

With DARPA support, Lincoln Laboratory developed a rugged and compact 3D imaging lidar system that has successfully demonstrated the feasibility and utility of this application. The sensor system was integrated into a UH-1 helicopter and demonstrated in both winter and summer flight campaigns. The sensor can operate either day or night and produces high-resolution 3D spatial images by using short laser pulses and a focal-plane array of Geiger-mode APD detectors with independent digital time-of-flight counting circuits at each pixel. The Jigsaw sensor technology includes Lincoln Laboratory developments of the microchip laser and novel photon-counting focal-plane arrays.

We employed a diffractive optical element to transform the single-mode laser beam into a 32×32 spot pattern. This approach results in high optical coupling efficiency of transmit and receive optical power while minimizing the background flux and false-alarm rate. The opto-mechanical design was engineered to maintain the alignment of these “spots and dots” through challenging thermal and vibration environments. The

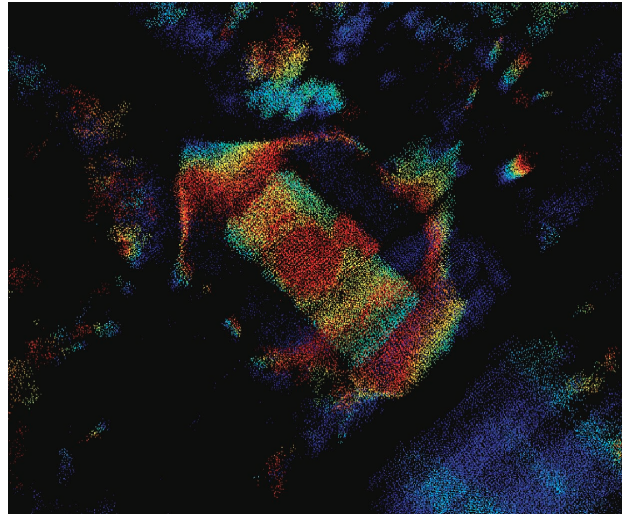


FIGURE 16. A subset of the same point-cloud data shown in the center of Figure 15. Compressing the color bar further reveals a military vehicle under the summer tree foliage and underneath the camouflage net. The spatial structure of the vehicle can now be used for identification.

development under a demanding schedule deadline was facilitated by the use of rapid prototyping techniques.

After limited laboratory checkout tests, the sensor system was shipped to Redstone Arsenal for integration into the UH-1 helicopter flight-test platform. The sensor head was integrated into a thirty-inch-diameter four-axis gimbal and the electronics rack was mounted inside the body of the helicopter, along with the government-provided gimbal controller and targeting computer. The Jigsaw system was used to collect imagery of ground vehicles both in the open and under foliage and camouflage obscurants.

Looking to the future, the Jigsaw team is investigating miniaturized versions of the sensor and electronics for application to small UAVs. During the next phase of the Jigsaw effort such a sensor will be demonstrated on a semi-autonomous unmanned flying platform.

Acknowledgments

The authors would like to recognize and acknowledge the contributions from many people who made this work possible. Many thanks to Robert O. Hauge and Lt. Col. Jack McCrae for their support and determination as the DARPA program managers; to Richard M. Heinrichs and John D. Shelton for their expert technical and management guidance and leadership; and to

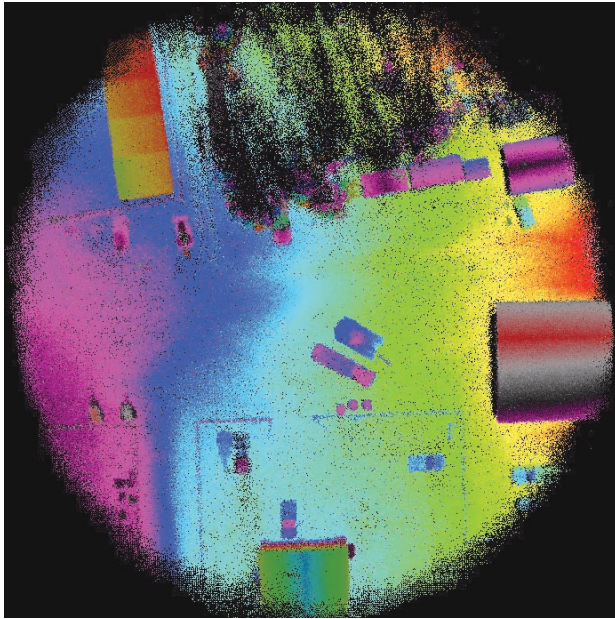


FIGURE 17. 3D image of tank yard, recorded with the sensor at an altitude of 450 m above ground level. The angular field of regard provided by the Risley scanner is 11°, but it covers an area about 85 m in diameter at this altitude. The scene includes several ground vehicles, fences, small sheds, and some buildings. The topology of the ground can be derived from the contours of the color bands.

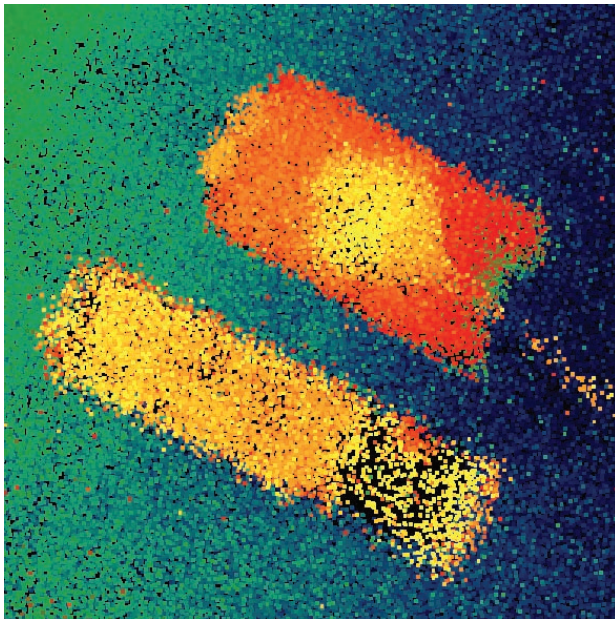


FIGURE 18. A close-up view of two ground vehicles from the tank-yard image in Figure 17. The data from this collection were processed with a spatial resolution of approximately 45 cm. Even at this reduced resolution, one vehicle can be classified as tank-like and the other as truck-like.

the many contributors from the Laboratory Engineering division who designed, fabricated, assembled, and tested the sensor system. We especially thank Gary Rich, Joseph L. McLaughlin, Jamie Burnside, Byron Stanley, Timothy Stephens, Eui-In Lee, Benjamin Chen, and David Ruscak; Dan Fouche, Greg Rowe, Robert Hatch, James Mooney, Mike O'Brien, Ted Square, Luke Skelly, Robert Garnier, Dave Ireland, Joseph Adams, Alex Vasile, and the Laser and Sensor Applications group; John Zayhowski and the Quantum Electronics group for the microchip laser subsystem; and Andy Loomis and Brian Aull and the Advanced Imaging Technology group for the remarkable focal-plane arrays.

We give special thanks to Joseph Grobmyer, Tommy Lum, Bill Cruger, and Tim Ricks and their team for excellent flight test and range support at Redstone Technical Test Center, Huntsville, Alabama. Finally, while this article is focused on the Lincoln Laboratory contributions, we also want to acknowledge our Jigsaw team members: Steve Hsu of Sarnoff Corporation; and Steve Blask, Van Reynolds, Joanne Pfannenstiel, Steve Campbell, and Dick Cannata from Harris Corporation.

REFERENCES

1. "2000 Army Science Board FY2000 Summer Study: Technical and Tactical Opportunities for Revolutionary Advancements in Rapidly Deployable Joint Ground Forces in the 2015–2025 Era," Army Science Board, Washington, D.C.
2. A.G. Gschwendtner and W.E. Keicher, "Development of Coherent Laser Radar at Lincoln Laboratory," *Linc. Lab. J.* 12 (2), 2000, pp. 383–396.
3. B.F. Aull, A.H. Loomis, D.J. Young, R.M. Heinrichs, B.J. Felton, P.J. Daniels, and D.J. Landers, "Geiger-Mode Avalanche Photodiodes for Three-Dimensional Imaging" *Linc. Lab. J.* 13 (2), 2002, pp. 335–350.
4. M.A. Albota, B.F. Aull, D.G. Fouche, R.M. Heinrichs, D.G. Kocher, R.M. Marino, J.G. Mooney, N.R. Newbury, M.E. O'Brien, B.E. Player, B.C. Willard, and J.J. Zayhowski, "Three-Dimensional Imaging Laser Radars with Geiger-Mode Avalanche Photodiode Arrays," *Linc. Lab. J.* 13 (2), 2002, pp. 351–370.
5. R.M. Marino, T. Stephens, R.E. Hatch, J.L. McLaughlin, J.G. Mooney, M.E. O'Brien, G.S. Rowe, J.S. Adams, L. Skelly, R.C. Knowlton, S.E. Forman, and W.R. Davis, "A Compact 3D Imaging Laser Radar System Using Geiger-Mode APD Arrays: System and Measurements," *SPIE* 5086, 2003, pp. 1–15.
6. A.C. van den Broek, R.J. Dekker, and P. Steeghs, "Robustness of Features for Automatic Target Discrimination in High-Resolution Polarimetric SAR Data," *SPIE* 5095, 2003, pp. 242–253.



RICHARD M. MARINO is a senior staff member in the Active Optical Systems group. He received a B.S. degree in physics from Cleveland State University, and an M.S. degree in physics and a Ph.D. degree in high-energy physics from Case Western Reserve University. He joined Lincoln Laboratory as a staff member in the Laser Radar Measurements group, and later joined the Systems and Analysis group. One of his most significant achievements has been his pioneering leadership in the development of a 3D imaging laser radar with photon-counting sensitivity. He has also worked at the Millimeter Wave Radar (MMW) and the ARPA-Lincoln C-band Observables Radar at the Kwajalein Missile Range in the Marshall Islands. While there, he was a mission test director at MMW and worked on range modernization plans. In 1997 he joined the Sensor Technology and Systems group of the Aerospace division and relocated its Silver Spring, Maryland, location to join the National Polar-Orbiting Operational Environmental Satellite System (NPOESS)/Integrated Program Office (IPO). At the IPO, he was lead technical advisor for the NPOESS Cross-Track Infrared Atmospheric Sounder Instrument (CrIs). He returned to Lincoln Laboratory in Lexington in 1999 and is again working on the development of 3D imaging laser-radar systems.



WILLIAM R. DAVIS, JR. is the assistant head of the Engineering division. He joined the Laboratory in 1977 after spending four years in the U.S. Air Force developing airborne high-energy laser systems, working principally in structural dynamics and beam pointing. At Lincoln Laboratory, he continued his work in high-energy laser systems, including beam control for missile defense applications. He managed the development of expendable radio frequency (RF) and infrared countermeasures that protect aircraft against missile threats, and he participated in the development of reentry decoys for ballistic missiles. He managed several studies concerning spacecraft and unmanned air vehicles as well as the Laboratory's pioneering efforts in micro air vehicles. More recently, he has worked on the development of airborne and space imaging laser radars. Throughout his career he has been involved in flight testing, conducting measurements, and qualifying payloads for a variety of aircraft. He received a B.S. degree in engineering mechanics from Lehigh University, and S.M. and Sc.D. degrees in aeronautics and astronautics from MIT.